Accounting for the variability in 3D interlock fabric permeability through fluid flow simulations

Morgan Cataldi, Yanneck Wielhorski, Nicolas Moulin, Monica Francesca Pucci, Pierre-Jacques Liotier

HAL Id: emse-04593308
https://hal-emse.ccsd.cnrs.fr/emse-04593308

Submitted on 29 May 2024

ACCOUNTING FOR THE VARIABILITY IN 3D INTERLOCK FABRIC PERMEABILITY THROUGH FLUID FLOW SIMULATIONS

Morgan Cataldi [a,b], Yanneck Wielhorski [b], Nicolas Moulin [a], Monica Francesca Pucci [c], Pierre-Jacques Liotier [d]

a: Mines Saint-Étienne, Univ Lyon, CNRS, UMR 5307 LGF, 158 Cours Fauriel 42023, Saint-Étienne, France – morgan.cataldi@emse.fr
b: Safran Aircraft Engines, Rond-point René Ravaud, Réau, 77550 Moissy-Cramayel, France
c: IMT Mines Alès, Univ Montpellier, LMGC CNRS, 6 Avenue de Clavières 30100, Alès, France
d: IMT Mines Alès, Univ Montpellier, PCH, 6 Avenue de Clavières 30100, Alès, France

Abstract: *Resin Transfer Moulding (RTM) processes used to manufacture high performance composite parts require an estimation of the fabric permeability and its variability. The value given to a constant intra-yarn permeability is thus a key parameter among many others studied in literature. To go further, the effect of variability into the intra-yarn permeability field onto 3D interlock fabric permeability is investigated. Reinforcements unit cells are modelled through material forming simulations which provide an intra-yarn fibre volume fraction (iy-FVF) field. The latter is used to locally compute an intra-yarn transversely isotropic permeability tensor field. Numerical simulations of dual-scale Stokes-Darcy coupled fluid flows between and within the yarns are performed with a monolithic approach by a Finite Element Method (FEM).*

Keywords: 3D interlock fabric; numerical permeability; intra-yarn permeability distribution; flow simulations; Stokes-Darcy coupling

1. Introduction

3D interlock fabrics are filled with an organic resin through RTM (Resin Transfer Moulding) processes to create high performance composite materials with designed mechanical properties. Due to their light weight compared to their mechanical properties, they are well suited for aeronautics. Ensuring composites mechanical properties implies a precise monitoring of the manufacturing. The fabric permeability is a key parameter of this process and thus needs to be characterised accurately. Fluid flow experiments or simulations within the fabric can be performed to compute its permeability. However, such a value comes along with its associated variability resulting from many factors. Among them, the variability of the intra-yarn permeability is of particular interest, since the weaved yarns are also porous materials which permeability is linked to its fibres local microstructure.

3D woven models generation [4-5] is widely used in the literature, and our simulations are performed on these models. Some works on the effect of the intra-yarn permeability onto the overall one have been conducted on whether idealized woven patterns as in Wang et al. [1] or X-ray micro-tomographies as in Ali et al. [2]. In such cases, a constant permeability tensor is generally given to all the yarns as in Geoffre et al. [3]. However, the yarns undergo a local compaction during the simulation of the forming process of the fabric. Consequently, the intra-yarn fibre volume fraction (iy-FVF) is locally computed all along the yarns, thus allowing the

calculation of an intra-yarn permeability field. The effect of its variability, induced by the fabric forming process, on the overall fabric permeability is studied.

The dual-scale fluid flow problem within and between the yarns can be modelled in several ways. Among them, Brinkman equation [6] is generally convenient to use through giving a very high artificial permeability value to the free space between the porous media [7-8]. In our simulations, the fluid flow is modelled by the Stokes-Darcy coupled problem and solved by a mixed velocity – pressure Finite Element (FE) formulation with a monolithic approach, which is detailed in previous works [9]. Its stability is ensured by a Variationnal Multiscale Method (VMS) named Algebraic SubGrid Scale (ASGS) method.

2.   Materials and Methods

2.1 Materials

The material used is a 3D angle-interlock woven fabric simulated with the software Multifil [10]. The unit cell is composed of 27 yarns and its dimensions are 18.9 x 18.9 x 4.9 (mm^3). This 3D fabric is computed with the woven pattern and the yarn features (the number of carbon fibres per yarn, their mechanical properties and their twist) as inputs. The yarn deformations are then computed by taking into account an enriched kinematics beam model and contact-friction interactions. Finally, the output unit cell contains both the meso-scale yarn morphology and the iy-FVF field which up-scales the microscopic intra-yarn morphology as shown in Figure 1. Yarns are described as consecutive sections attached and oriented along their neutral fibres.
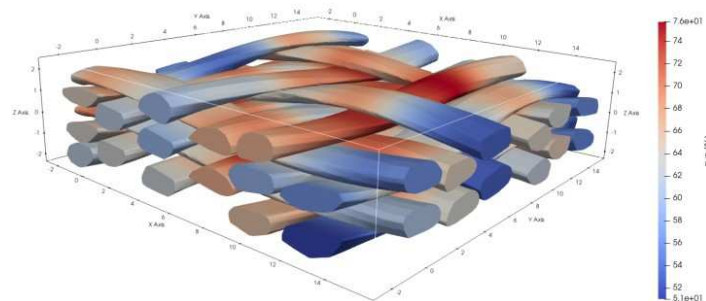

Figure 1. 3D interlock unit cell and its iy-FVF field

The unit cell thus describes the fabric at the mesoscopic scale where yarns are homogeneous porous media characterized by a permeability tensor. This allows considering both flow scales: within (microscopic scale) and between (mesoscopic scale) the yarns. The intra-yarn permeability tensor is assumed transversely isotropic and described in its principal coordinate system shown in Figure 2 by its eigenvalues K_I, K_{II} and K_{III}.
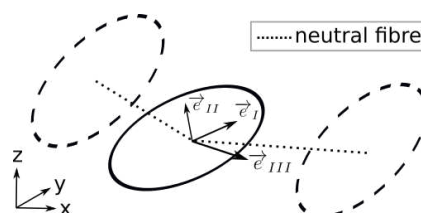

Figure 2. Coordinate system of a yarn section, with K_I, K_{II} and K_{III} its permeability components

Then, their numerical values can be calculated from a iy-FVF value V_f through the Gebart's law (Eq. (1) and (2), with the fibre radius R = 2.6e-3 mm), detailed in [11], for transverse $K_I = K_{II} = K_T$ and longitudinal $K_{III} = K_L$ permeabilities in relation to fibre orientation in a hexagonal arrangement. The mean values of K_T and K_L are respectively 2.03e-14 m^2 and 9.73e-14 m^2.

$$K_T = \frac{16R^2}{9\pi\sqrt{2}}\left(\sqrt{\frac{\pi}{2\sqrt{3}V_f}} - 1\right)^{2.5}$$

(1)

$$K_L = \frac{8R^2}{53}\frac{(1 - V_f)^3}{V_f^2}$$

(2)

The fluid injected within the preform is supposed to have a Newtonian behaviour and its dynamic viscosity is set to a constant value of μ = 0.2 Pa.s for all simulations performed in the present work. This value corresponds to the dynamic viscosity at 120°C of an epoxy resin.

2.2 Methods

The following steps are needed to compute the permeability of the previous unit cell. Firstly, it has to be meshed with tetrahedra and that should have conformal interfaces between Stokes (inter-yarn region) and Darcy (intra-yarn region). Then, finite element simulations of the dual-scale steady-state fluid flow within it are performed. Finally, the resulting velocity and pressure fields are post-processed to compute the homogenized permeability of the unit cell.

Both yarns and spaces between them are meshed with tetrahedra forming an unstructured grid. This kind of mesh was chosen instead of a structured grid because it allows to mesh more efficiently complex geometries such as those involved in this work. The unit cell is firstly meshed with voxels [12-13], and then remeshed by Mirax with tetrahedra [14]. Moreover, the mesh is conformal, meaning that nodes belonging to elements from both parts of an interface are matching on the interface itself. So, this feature allows an explicit description of the different regions within the unit cell. The results of both steps are shown in Figure 3. The characteristic size of the voxels is 100 μm, thus leading to a tetrahedral mesh with 2.8 million nodes and 16 million elements.

(a) *(b)*

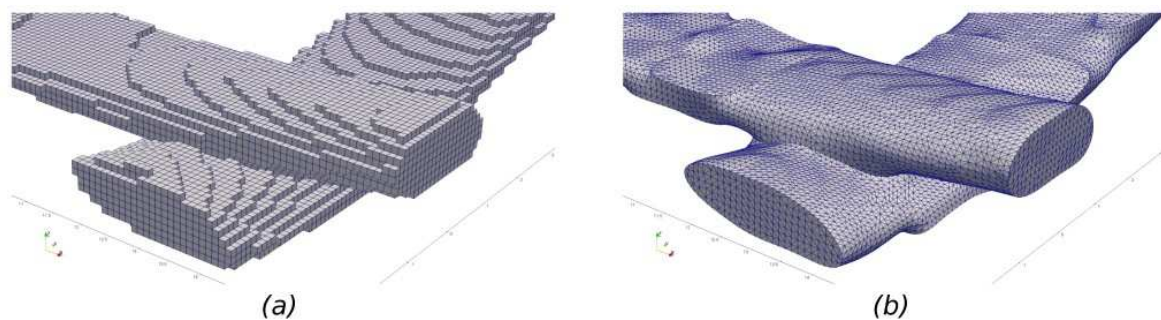*Figure 3. Meshed 3D interlock unit cell with voxels (a) and tetrahedra (b)*

Finite element simulations are performed with the Z-set software [15]. The steady-state fluid flow is modelled as incompressible and laminar (*ie:* for small Reynolds numbers Re<<1). The fluid has a Newtonian behaviour with a constant dynamic viscosity. The fluid flow within the inter-yarn domain is then modelled by the Stokes problem shown in Eq. (3).

$$\begin{cases} \mu \Delta \vec{v} = \vec{\nabla} p \\ \vec{\nabla} . \vec{v} = 0 \end{cases} \tag{3}$$

Whereas the yarns are assumed to be porous and considered as homogeneous equivalent media. Hence, they can be characterized by a permeability tensor and fluid flow within the yarns is modelled by the Darcy problem as follows Eq. (4).

$$\begin{cases} \vec{v} = -\frac{1}{\mu} \underline{\underline{K}} . \vec{\nabla} p \\ \vec{\nabla} . \vec{v} = 0 \end{cases} \tag{4}$$

The fluid flow problem on the whole domain is then modelled by the coupled Stokes-Darcy problem. A mixed velocity-pressure finite element formulation is used through the entire unit cell and P1/P1 elements are used to approximate piecewise linearly both velocity and pressure fields. Such formulation is not stable, so Variational Multi-Scale (VMS) method, especially the Algebraic Sub-Grid Scale (ASGS) technique, is used to stabilise the coupled problem. Moreover, one simulation per direction needs to be performed to compute the effective permeability tensor of the unit cell. A pressure drop $\Delta P = P_e - P_s$ is applied respectively in the X, Y and Z directions, while for the other unit cell boundaries a null normal velocity condition is given, as shown in Figure 4. Note that no periodic boundary condition can be applied on this unit cell since it is not periodic. The pressure values assigned in this work are $P_e = 1$ Pa and $P_s = 0$ Pa.
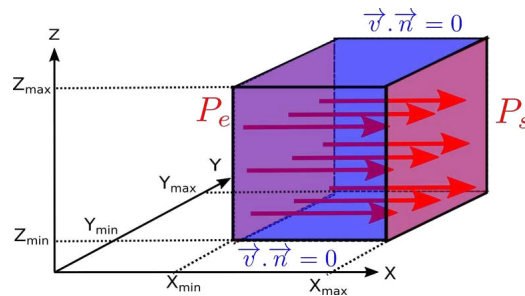

Figure 4. Boundary conditions applied on the unit cell for a main flow in the X direction

The effective permeability of the unit cell is post-processed through the 3D-generalized Darcy law shown in Eq. (4) by using the software Paraview [16]. No assumptions are made on this tensor, so all its components are computed. All the flow rate values involved are computed by integrating the velocity field component normal to the planes of abscissa $X = X_{max}$, $Y = Y_{max}$ and $Z = Z_{max}$ respectively. All the pressure values involved are computed as the mean value of the pressure over the corresponding unit cell boundary.

3. Results

3.1 Pressure and velocity fields resulting from the simulations

Finite element simulations of the fluid flow along the three main directions X, Y and Z have been performed. The resulting pressure and velocity fields for a main flow along the X direction are shown in Figure 5. The pressure field decreases linearly in average through the unit cell but with local variations due to the intra-yarn permeability. Differences in the velocity field highlight the global alignment of velocity vectors with the main flow direction. The fluid velocity has an average of 1.4e-2 mm.s^{-1} in our simulations, with those specific boundary

conditions. Nonetheless, the numerical permeability computed from a steady-state flow should not depend on the fluid velocity.
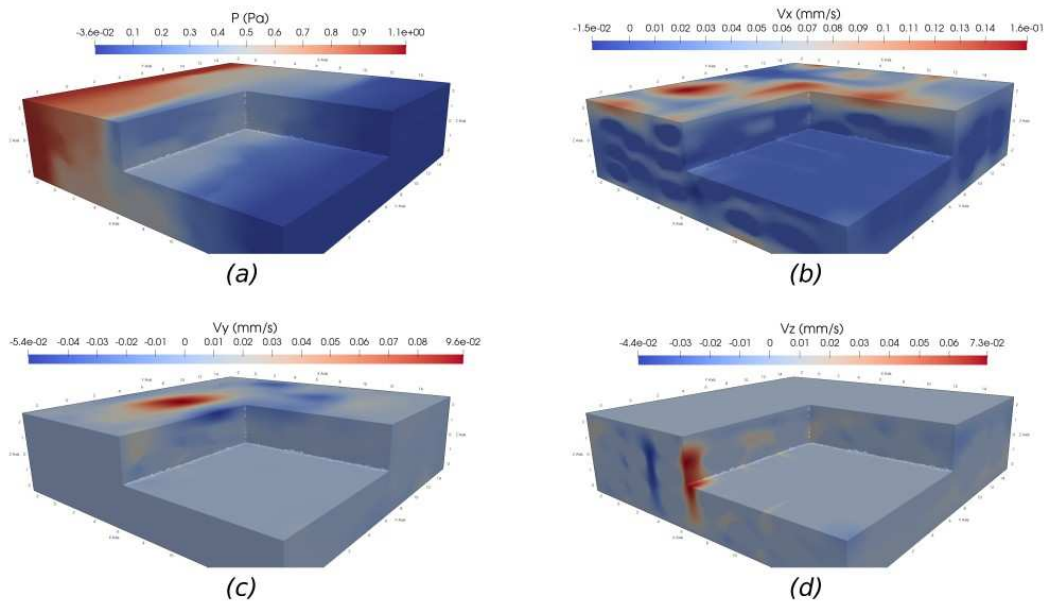

(a)

(b)

(c)

(d)

Figure 5. (a) pressure and velocity fields - (b) v_x, (c) v_y and (d) v_z - for a main flow in the X direction

However, preferential flow channels located close to the unit cell boundaries will lead to an overestimation of the fabric numerical permeability. This phenomenon is intrinsic to our mesoscopic unit cell and so it has the same significance for all the present simulations. Still, the results obtained in this first approach cannot be easily extended to unit cells without preferential flow channels.

It is also interesting to have a look at flow paths to get a qualitative idea of the balance between the inter- and intra-yarn flows. Figure 6 shows that most of the streamlines flow around the yarns and do not penetrate them. This can be explained by the relatively low yarns permeabilities compared to the relatively wide flow channels between them. Nevertheless, some streamlines penetrate the yarns, but with much smaller velocities. Therefore, the inter-yarn meso-scale flow is more significant in our unit cell than the intra-yarn micro-scale flow. Thus, the fabric permeability is mainly determined by its meso-scale morphology than by its intra-yarn permeabilities.
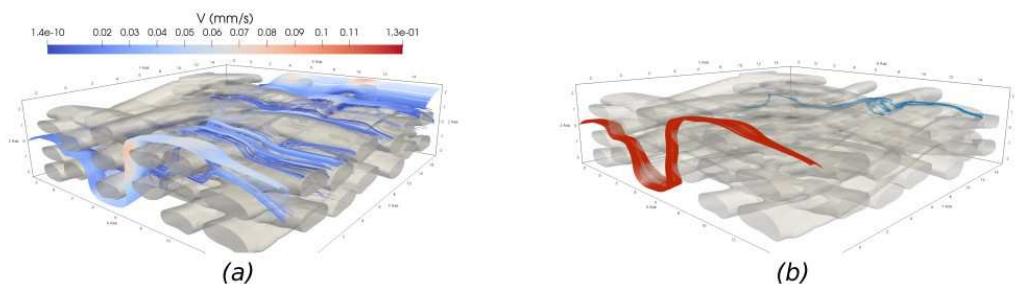

(a)

(b)

Figure 6. Streamlines from the inlet boundary X = X_{min} at Z = 0 mm: (a) all the streamlines and (b) a non-penetrating group (red) and a penetrating group (blue) of streamlines

3.2 Effect of the intra-yarn fiber volume fraction field variability on the fabric permeability

A fibre volume fraction is used to characterise each yarn section. This leads to a higher level of details on the micro-scale yarn characteristics. This field has been averaged for each yarn, thus giving a iy-FVF value per yarn, but also averaged over all the yarns, thus giving a global iy-FVF value for all the yarns, see Figure 7. The aim is to investigate how much the iy-FVF field level of definition changes the fabric permeability. Then the permeability tensor is calculated through Gebart's laws as explained previously, the finite element simulations are performed, and the computed fabric permeability tensors are expressed in Eq. (5) in m^2.
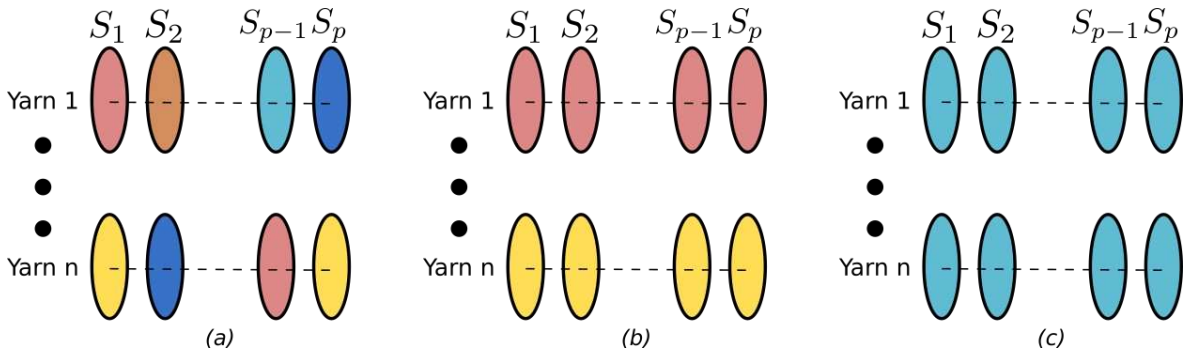

Figure 7. *iy-FVF field levels of definition (colors representing different iy-FVF values): (a) section, (b) yarn and (c) global*

$$\underline{\underline{K}}_{section} = \begin{pmatrix} 5.65 \times 10^{-8} & -5.80 \times 10^{-10} & -2.16 \times 10^{-10} \\ -1.77 \times 10^{-9} & 8.80 \times 10^{-8} & -5.11 \times 10^{-10} \\ -6.11 \times 10^{-9} & 3.51 \times 10^{-9} & 2.19 \times 10^{-8} \end{pmatrix}$$
$$\underline{\underline{K}}_{yarn} = \begin{pmatrix} 5.65 \times 10^{-8} & -5.80 \times 10^{-10} & -2.15 \times 10^{-10} \\ -1.77 \times 10^{-9} & 8.80 \times 10^{-8} & -5.13 \times 10^{-10} \\ -6.11 \times 10^{-9} & 3.51 \times 10^{-9} & 2.19 \times 10^{-8} \end{pmatrix} \qquad (5)$$
$$\underline{\underline{K}}_{global} = \begin{pmatrix} 5.65 \times 10^{-8} & -5.79 \times 10^{-10} & -2.14 \times 10^{-10} \\ -1.77 \times 10^{-9} & 8.80 \times 10^{-8} & -5.15 \times 10^{-10} \\ -6.11 \times 10^{-9} & 3.51 \times 10^{-9} & 2.19 \times 10^{-8} \end{pmatrix}$$

It appears that the computedfabric permeability tensors are diagonally dominant since their non-diagonal terms are one or two orders of magnitude smaller than their diagonal terms. Computation of the tensors eigenvectors supports the idea that their principal directions are well aligned with the fabric directions X, Y and Z. The relative difference between the permeability tensors with regards to a iy-FVF field defined per yarn section is computed by Eq. (6) by using the spectral norm defined in Eq. (7), where ρ is the spectral radius of the tensor.

$$\frac{\left\| \underline{\underline{K}}_i - \underline{\underline{K}}_{section} \right\|_{2,2}}{\left\| \underline{\underline{K}}_{section} \right\|_{2,2}} \quad \text{with:} \quad i \in \{yarn, global\} \qquad (6)$$

$$\left\| \underline{\underline{K}} \right\|_{2,2} = \sup_{\|\vec{x}\|_2 \leq 1} \left\| \underline{\underline{K}} \vec{x} \right\|_2 = \sqrt{\rho \left({}^t\underline{\underline{K}}\,\underline{\underline{K}} \right)} \qquad (7)$$

The result is a relative difference of 2.54e-5 and 5.10e-5 for the yarn and global iy-FVF definition levels respectively. So, there is no meaningful effect of the iy-FVF field variability on our unit cell permeability. An explanation can come from the analysis of the flow paths, which conclusion was that the fabric permeability is more affected by its meso-scale morphology

than by its iy-FVF field, and so by its intra-yarn permeability field. As such, intra-yarn characteristics variability is of little impact on the flow within the unit cell, and so on the fabric permeability.

This result is applicable only in the particular conditions of this first approach which are: unit cells with preferential flow channels and a steady-state flow. Consequently, a first area to investigate in the future would be unsaturated flows. The variability of intra-yarn characteristics on the flow paths and the filling time is thought to be more impacting in such cases than in steady-state flows. The second area would be to study the same unit cell, but truncated, hence avoiding the preferential flow channels. Moreover, different unit cells corresponding to several compaction levels of the same fabric will be investigated. This allows to change the contribution ratio of the micro-scale flow compared to the meso-scale flow by reducing the inter-yarn space in whole the unit cell related to the compaction level.

4. Conclusion

Finite element simulations of the dual-scale flow within a 3D interlock unit cell were performed in order to compute the fabric permeability tensor without prior assumptions made on its nature. The Stokes-Darcy coupled problem was solved by a monolithic approach stabilized by the ASGS method. The unit cell resulting from a material forming simulation is described at the meso-scale by its yarns morphology, and at the micro-scale by an intra-yarn fibre volume fraction field. The latter was averaged in two steps in order to investigate the effect of its variability, and thus the intra-yarn permeability field variability, on the fabric permeability tensor. The result is that there is no meaningful impact for the unit cell studied here, which has some preferential flow channels. These are thought to increase the weight of the meso-scale inter-yarn flow compared to the micro-scale intra-yarn flow. That is why further works will broaden this study to 3D interlock unit cells without preferential flow channels. The aim is more widely to explore different relative weights of meso- and micro-scale flows in order to observe in what cases the iy-FVF field variability affects the fabric permeability. Afterwards, such study will be extended to unsaturated flows.

5. References

1. Wang Q., Mazé B., Tafreshi HV., Pourdeyhimi B. A note on permeability simulation of multifilament woven fabrics. Chemical Engineering Science. 2006 dec; 61 (24).
2. Ali MA., Umer R., Khan KA., Cantwell WJ. XCT-scan assisted flow path analysis and permeability prediction of a 3D woven fabric. Composites Part B: Engineering. 2019 nov; 176.
3. Geoffre A., Wielhorski Y., Moulin N., Bruchon J., Drapier S., Liotier PJ. Influence of intra-yarn flows on whole 3D woven fabric numerical permeability: from Stokes to Stokes-Darcy simulations. International Journal of Multiphase Flow. 2020 aug; 129.
4. Wielhorski Y., Mendoza A., Rubino M., Roux S. Numerical modeling of 3D woven composite reinforcements: A review. Composites Part A: Applied Science and Manufacturing. 2022 mar; 154.
5. Lomov SV., Huysmans G., Luo Y., Parnas RS., Prodromou A., Verpoest I., et al. Textile composites: modelling strategies. Composites Part A: Applied Science and Manufacturing. 2001 oct; 32 (10).

6. Brinkman HC. A calculation of the viscous force exerted by a flowing fluid on a dense swarm of particles. Flow, Turbulence and Combustion. 1949 dec; 1 (1).

7. Shou D., Ye L., Tang Y., Fan J., Ding F. Transverse permeability determination of dual-scale fibrous materials. International Journal of Heat and Mass Transfer. 2013 mar; 58 (1-2).

8. Syerko E., Binetruy C., Comas-Cardona S., Leygue A. A numerical approach to design dual-scale porosity composite reinforcements with enhanced permeability. Materials & Design. 2017 oct; 131.

9. Abou Orm L., Troian R., Drapier S., Bruchon J., Moulin N. Stokes–Darcy coupling in severe regimes using multiscale stabilisation for mixed finite elements: monolithic approach versus decoupled approach. European Journal of Computational Mechanics. 2014 jul; 23 (3-4).

10. Durville D., Baydoun I., Moustacas H., Périé G., Wielhorski Y. Determining the initial configuration and characterizing the mechanical properties of 3D angle-interlock fabrics using finite element simulation. International Journal of Solids and Structures. 2018 dec; 154.

11. Gebart BR. Permeability of Unidirectional Reinforcements for RTM. Journal of Composite Materials. 1992 aug; 26 (8).

12. Schneider J., Hello G., Aboura Z., Benzeggagh M., Marsal D. A meso-fe voxel model of an interlock woven composite. In: Proceeding of the international conference in composite materials 17th (ICCM17), Edinburgh, Scotland; 2009.

13. Hello G., Schneider J., Aboura Z. Numerical simulations of woven composite materials with voxel-fe models. In: Proceedings of the 16th European Conference on Composite Materials; 2014. p.22–26.

14. Rassineux A. Robust conformal adaptive meshing of complex textile composites unit cells. Composite Structures. 2022 jan; 279.

15. Missoum-Benziane D., Chiaruttini V., Garaud JD., Feyel F., Foerch R., Osipov N., et al. Z-set/ZeBuLoN : une suite logicielle pour la mécanique des matériaux et le calcul de structures. In: 10e colloque national en calcul des structures. Giens, France; 2011. p.8.

16. Ahrens J., Geveci B., Law C. Paraview: An end-user tool for large data visualization. The visualization handbook. 2005; 717 (8).